Journal of Applied Mathematics and Physics, 2023, 11, 69-84
https://www.scirp.org/journal/jamp
ISSN Online: 2327-4379
ISSN Print: 2327-4352

Determination of Solar Radius and Earth's Radius by Relativistic Matter Wave

Huaiyang Cui

Department of Physics, Beihang University, Beijing, China
Email: hycui@buaa.edu.cn

How to cite this paper: Cui, H.Y. (2023) Determination of Solar Radius and Earth's Radius by Relativistic Matter Wave. *Journal of Applied Mathematics and Physics*, **11**, 69-84.
https://doi.org/10.4236/jamp.2023.111006

Received: November 30, 2022
Accepted: January 15, 2023
Published: January 18, 2023

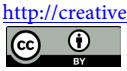

Abstract

In recent years, relativistic matter waves have been applied to the solar system to explain some quantum gravity effects. This paper shows that the solar size and Earth's size are the consequences of Bode's rule in terms of the relativistic matter wave. The solar radius is determined as 7e+8 (m) with a relative error of 0.72%; the Earth's radius is determined as 6.4328e+6 (m) with a relative error of 0.86%. The Earth's atmospheric circulation is also investigated in terms of the relativistic matter wave, the wind fields on the Earth's surface are calculated, and the results agree well with experimental observation. These findings indicate that the solar system is under the control of the planetary relativistic matter waves.

Keywords

Relativistic Matter Wave, Sunspot Cycle, Atmospheric Circulation

1. Introduction

In general, some quantum gravity proposals [1] [2] are extremely hard to test in practice, as quantum gravitational effects are appreciable only at the Planck scale [3]. However, Bode's rule provides another scheme to deal with quantum gravity effects.

A quantization pattern in the solar system is known today as Bode's rule, pointed out in 1766 [4], it agrees well with the distances of the planets from the Sun, as shown in Table 1.

Since Bode's rule holds, there must exist a planetary wave called as **relativistic matter wave** [5] [6] [7] to support its quantization pattern. Here, we show that the solar size and Earth's size are also the consequence of Bode's rule in terms of the relativistic matter wave; the results are consistent with the general description of the star's interior [8]-[15].

Table 1. Bode' rule and predictions.

Planet	True Distance	Bode's Rule	Prediction of Relativistic Matter Wave
Mercury	0.39	(0 + 4)/10 = 0.4	0.375
Venus	0.72	(3 + 4)/10 = 0.7	0.667
Earth	1.00	(6 + 4)/10 = 1.0	1.04
Mars	1.52	(12 + 4)/10 = 1.6	1.50
Ceres (dwarf)	2.78	(24 + 4)/10 = 2.8	
Jupiter	5.20	(48 + 4)/10 = 5.2	
Saturn	9.58	(96 + 4)/10 = 10	
Uranus	19.2	(192 + 4)/10 = 19.6	
Neptune	39.5	(384 + 4)/10 = 38.8	

2. Bode's Rule and Relativistic Matter Wave

The relativistic matter wave [7] is given by

$$\psi = \exp\left(\frac{i\beta}{c^3}\int_0^x \left(u_1 \mathrm{d}x_1 + u_2 \mathrm{d}x_2 + u_3 \mathrm{d}x_3 + u_4 \mathrm{d}x_4\right)\right) \tag{1}$$

where u is 4-velocity of planet, β is a constant determined by experiments. As shown in **Figure 1(a)**, the planetary circular orbit can be quantized as

$$\left.\begin{array}{l} \dfrac{\beta}{c^3}\oint_L v_l \mathrm{d}l = 2\pi n \\ v_l = \sqrt{\dfrac{GM}{r}} \end{array}\right\} \Rightarrow \sqrt{r} = \frac{c^3}{\beta\sqrt{GM}} n; \quad n = 0,1,2,\cdots \tag{2}$$

This orbital quantization equation coincides well with the Bode' rule for those inner planets in the solar system, as listed in **Table 1**, as shown in **Figure 1(b)**.

In **Figure 1(b)**, the blue straight line expresses a linear regression relation among the Sun, Mercury, Venus, Earth and Mars, so it gives β = 2.961520e+10 (m/s^2). In accordance with the Bode's rule, quantum numbers n = 3, 4, 5, … were assigned to the solar planets, the Sun was assigned a quantum number n = 0 because the Sun is in the **central state**.

3. Determining the Solar Density and Radius by the Bode's Rule

The Bode's rule has been interpreted as the present relativistic matter wave. In a central state n = 0 with a size, if the coherent length of the relativistic matter wave is long enough, its head may overlap with its tail when the particle moves in a closed orbit in space-time, as shown in **Figure 1(a)**. The overlapped wave is given by

$$\begin{aligned} &\psi = \psi(r)T(t) \\ &\psi(r) = 1 + \mathrm{e}^{i\delta} + \mathrm{e}^{i2\delta} + \cdots + \mathrm{e}^{i(N-1)\delta} = \frac{1-\exp(iN\delta)}{1-\exp(i\delta)} \\ &\delta(r) = \frac{\beta}{c^3}\oint_L (v_l)\mathrm{d}l = \frac{2\pi\beta\omega r^2}{c^3} \end{aligned} \tag{3}$$

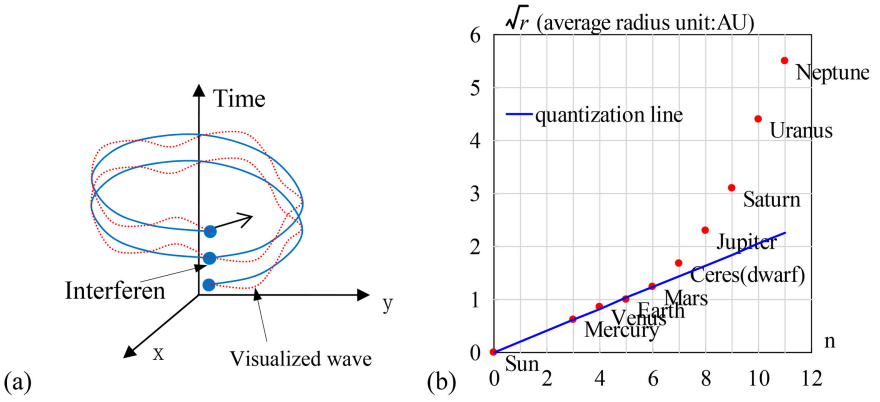

Figure 1. (a) The head of the relativistic matter wave may overlap with its tail; (b) The inner planets are quantized.

where N is the overlapping number which is determined by the coherent length of the relativistic matter wave, δ is the phase difference after one orbital motion, ω is the angular speed of the solar self-rotation. The above equation is a multi-slit interference formula in optics, for a larger N it is called as the Fabry-Perot interference formula.

The relativistic matter wave function ψ needs a further explanation. In quantum mechanics, $|\psi|^2$ equals to the probability of finding an electron due to Max Burn's explanation; in astrophysics, $|\psi|^2$ equals to the probability of finding a nucleon (proton or neutron) *averagely on an astronomic scale*, we have

$$|\psi|^2 \propto \text{nucleon-density} \propto \rho \tag{4}$$

It follows from the multi-slit interference formula that the overlapping number N is estimated by

$$N^2 = \frac{\left|\psi(0)_{\text{multi-wavelet}}\right|^2}{\left|\psi(0)_{\text{one-wavelet}}\right|^2} = \frac{\rho_{\text{core}}}{\rho_{\text{surface\_gas}}} \tag{5}$$

The solar core has a mean density of 1408 (kg/m^3), the surface of the Sun is comprised of convective zone with a mean density of 2e-3 (kg/m^3) [8]. In this paper, the Sun's radius is chosen at a location where density is 4e-3 (kg/m^3), thus the solar overlapping number N is calculated to be $N = 593$.

Sun's angular speed at its equator is known as $\omega = 2\pi/(25.05 \times 24 \times 3600)$ (s^{-1}). Its mass 1.9891e+30 (kg), well-known radius 6.95e+8 (m), mean density 1408 (kg/m^3), the constant β = 2.961520e+10 (m/s^2). According to the $N = 593$, the matter distribution of the $|\psi|^2$ is calculated in **Figure 2**, it agrees well with the general description of star's interior [8]-[15]. The radius of the Sun is determined as $r = 7e+8$ (m) with a relative error of 0.72% in **Figure 2**, which indicates that the Sun radius strongly depends on the Sun's self-rotation.

<Clet2020 Script>//C source code

```
int i,j,k,m,n,N,nP[10];
double beta,H,B,M,r,r_unit,x,y,z,delta,D[1000],S[1000], a,b,rs,rc,omega,
atm_height; char str[100];
```

```
main(){k=150;rs=6.95e8;rc=0;x=25.05;omega=2*PI/(x*24*3600);n=0;a=1408/
0.004; N=sqrt(a);
beta=2.961520e10;H=SPEEDC*SPEEDC*SPEEDC/beta;M=1.9891E30;
atm_height=2e6; r_unit=1E7;
for(i=-k;i<k;i+=1) {r=abs(i)*r_unit;
if(r<rs+atm_height) delta=2*PI*omega*r*r/H; else
delta=2*PI*sqrt(GRAVITYC*M*r)/H;//around the star
x=1;y=0; for(j=1;j<N;j+=1){z=delta*j; x+=cos(z);y+=sin(z);}z=x*x+y*y;
z=z/(N*N);
S[n]=i;S[n+1]=z; if(i>0 && rc== 0 && z<0.0001) rc=r; n+=2;}
SetAxis(X_AXIS,-k,0,k,"#ifr; ; ; ;");SetAxis(Y_AXIS,0,0,1.2,"#if|ψ|#su2#t;0;0.4;
0.8; 1.2;");
DrawFrame(FRAME_SCALE,1,0xafffaf); z=100*(rs-rc)/rs;
SetPen(1,0xff0000);Polyline(k+k,S,k/2,1," nucleon_density"); SetPen
(1,0x0000ff);
r=rs/r_unit;y=-0.05;D[0]=-r;D[1]=y;D[2]=r;D[3]=y;
Draw("ARROW,3,2,XY,10, 100,10,10,",D);
Format(str,"#ifN#t=%d#n#ifβ#t=%e#nrc=%e#nrs=%e#nerror=%.2f%",N,beta,
rc,rs,z);
TextHang(k/2,0.7,0,str);TextHang(r+5,y/2,0,"#ifr#sds#t");TextHang(-r,y+y,0,
"Sun diameter");
}#v07=?>A
```

4. Determining the Earth's Density and Radius by the Bode's Rule

The Bode's rule can be applied to the Earth and Moon. The Moon is assigned a quantum number of $n = 2$ because some quasi-satellite's perigees have reached a depth almost at $n = 1$ orbit, as shown in **Figure 3**. Here, the constant β = 1.377075e+14 (m/s^2) is determined uniquely by the line between the Earth and Moon by Equation (2).

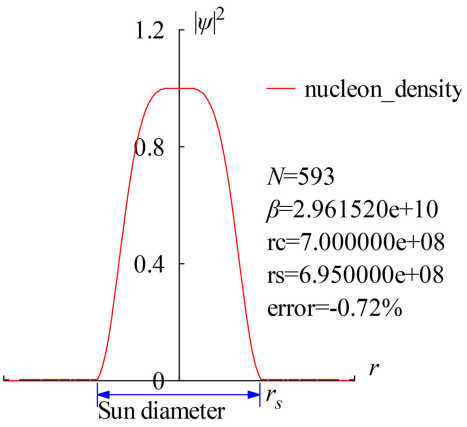

Figure 2. The nucleon distribution $|\psi|^2$ in the Sun is calculated in the radius direction.

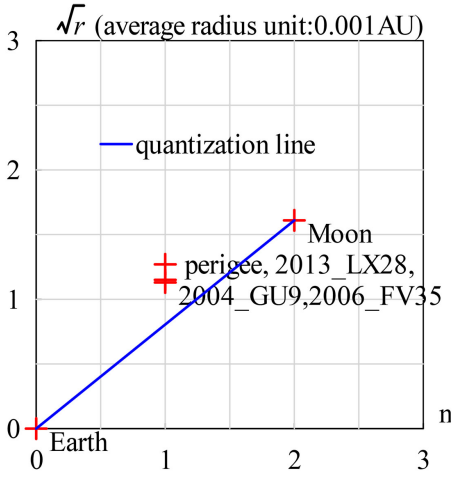

Figure 3. Orbital quantization for the Moon.

The Earth has a mean density of 5530 (kg/m^3), its surface is covered with air and vapor with a density of 1.29 (kg/m^3). The Earth's radius is chosen at the sea level, it follows Equation (5) that the Earth's overlapping number N is calculated to be $N = 65$.

The Earth's angular speed is known as $\omega = 2\pi/(24 \times 3600)$ (s^{-1}), its mass 5.97237e+24 (kg), the well-known radius is 6.371e+6 (m), the Earth constant $\beta =$ 1.377075e+14 (m/s^2). The matter distribution $|\psi|^2$ in radius direction is calculated by Equation (3), as shown in **Figure 4(a)**. The radius of the Earth is determined as $r = 6.4328e+6$ (m) with a relative error of 0.86%, it agrees well with common knowledge.

Space debris over the atmosphere has a complicated evolution [16] [17] [18], and has itself speed and phase

$$v_l = \sqrt{\frac{GM}{r}}; \quad \delta(r) = \frac{\beta}{c^3}\oint_L (v_l)\mathrm{d}l = \frac{2\pi\beta}{c^3}\sqrt{GMr} \tag{6}$$

The secondary peaks over the atmosphere up to 2000 km altitude are calculated in **Figure 4(b)** which agree well with the space debris observations [16]; the peak near 890 km altitude is due principally to the January 2007 intentional destruction of the FengYun-1C weather spacecraft, while the peak centered at approximately 770 km altitude was created by the February 2009 accidental collision of Iridium 33 (active) and Cosmos 2251 (derelict) communication spacecraft [18] [19] [20]. The observations based on the incoherent scattering radar EISCAT ESR located at 78˚N in Jul. 2006 and in Oct. 2015 [21] [22] [23] are respectively shown in **Figure 4(c)** and **Figure 4(d)**. This prediction of secondary peaks also agrees well with other space debris observations [24] [25].

<Clet2020 Script>//C source code

```
int i,j,k,m,n,N,nP[10]; double H,B,M,v_r,r,AU,r_unit,x,y,z,delta,D[10],S[1000];
double rs,rc,rot,a,b,atm_height,beta; char str[100];
main(){k=80;rs=6.378e6;rc=0;atm_height=1.5e5;n=0; N=65;
```

```
beta=1.377075e+14;H=SPEEDC*SPEEDC*SPEEDC/beta;
M=5.97237e24;AU=1.496E11;r_unit=1e-6*AU; rot=2*PI/(24*60*60);//angular speed of the Earth
for(i=-k;i<k;i+=1) {r=abs(i)*r_unit;
if(r<rs+atm_height) v_r=rot*r*r; else v_r=sqrt(GRAVITYC*M*r);//around the Earth
delta=2*PI* v_r/H; y=SumJob("SLIT_ADD,@N,@delta",D); y=y/(N*N);
if(y>1) y=1; S[n]=i;S[n+1]=y; if(i>0 && rc== 0 && y<0.001) rc=r; n+=2;}
SetAxis(X_AXIS,-k,0,k,"r; ; ; ;");SetAxis(Y_AXIS,0,0,1.2,"#if|ψ|#su2#t;0;0.4;0.8;1.2;");
DrawFrame(FRAME_SCALE,1,0xafffaf); x=50;z=100*(rs-rc)/rs;
SetPen(1,0xff0000);Polyline(k+k,S,k/2,1," nucleon_density");
r=rs/r_unit;y=-0.05;D[0]=-r;D[1]=y;D[2]=r;D[3]=y;
SetPen(2,0x0000ff); Draw("ARROW,3,2,XY,10,100,10,10,",D);
Format(str,"#ifN#t=%d#n#ifβ#t=%e#nrc=%e#nrs=%e#nerror=%.2f%",N,beta,rc,rs,z);
TextHang(k/2,0.7,0,str);TextHang(r+5,y/2,0,"r#sds#t");TextHang(-r,y+y,0,"Earth diameter");
}#v07=?>A#t
<Clet2020 Script>//C source code
int i,j,k,m,n,N,nP[10]; double H,B,M,v_r,r,AU,r_unit,x,y,z,delta,D[10],S[10000];
double rs,rc,rot,a,b,atm_height,p,T,R1,R2,R3; char str[100]; int Debris[96]={110,0,237,0,287,0,317,2,320,1,357,5,380,1,387,4,420,2,440,3,454,14,474,9,497,45,507,26,527,19,557,17,597,34,634,37,664,37,697,51,727,55,781,98,808,67,851,94,871,71,901,50,938,44,958,44,991,37,1028,21,1078,17,1148,10,1202,9,1225,6,1268,12,1302,9,1325,5,1395,7,1395,18,1415,36,1429,12,1469,22,1499,19,1529,9,1559,5,1656,4,1779,1,1976,1,};
main(){k=80;rs=6.378e6;rc=0;atm_height=1.5e5;n=0; N=65;
H=1.956611e11;M=5.97237e24;AU=1.496E11;r_unit=1e4;
rot=2*PI/(24*60*60);//angular speed of the Earth
b=PI/(2*PI*rot*rs*rs/H);
R1=rs/r_unit;R2=(rs+atm_height)/r_unit;R3=(rs+2e6)/r_unit;
for(i=R2;i<R3;i+=1) {r=abs(i)*r_unit; delta=2*PI*sqrt(GRAVITYC*M*r)/H;
y=SumJob("SLIT_ADD,@N,@delta",D); y=1e3*y/(N*N);//visualization scale:1000
if(y>1) y=1; S[n]=i;S[n+1]=y;n+=2;}
SetAxis(X_AXIS,R1,R1,R3,"altitude; r#sds#t;500;1000;1500;2000km ;");
SetAxis(Y_AXIS,0,0,1,"#if|ψ|#su2#t;0;  ;1e-3;");DrawFrame(FRAME_SCALE,1,0xafffaf); x=R1+(R3-R1)/5;
SetPen(1,0xff0000);Polyline(n/2,S,x,0.8,"#if|ψ|#su2#t (density, prediction)");
for(i=0;i<48;i+=1) {S[i+i]=R1+(R3-R1)*Debris[i+i]/2000; S[i+i+1]=Debris[i+i+1]/300;}
SetPen(1,0x0000ff);Polyline(48,S,x,0.7,"Space debris (2018, observation)"); }
#v07=?>A#t
```

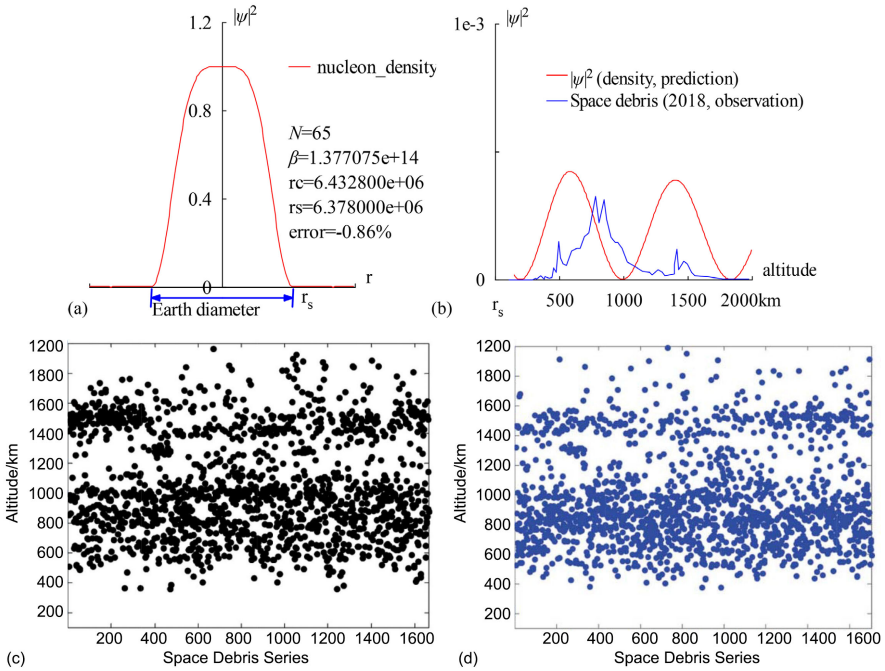

Figure 4. (a) The radius of the Earth is calculated out r = 6.4328e+6 (m) with a relative error of 0.86% by the interference of its relativistic matter wave; (b) The prediction of the space debris distribution up to 2000 km altitude; (c) The pace debris distribution in Jul. 2006, Joint observation based on the incoherent scattering radar EISCAT ESR located at 78˚N [21]; (d) The space debris distribution in Oct. 2015, Joint observation based on the incoherent scattering radar EISCAT ESR located at 78˚N [21].

5. Sunspot Cycle

The **coherence length** of waves is usually mentioned but the **coherence width** of waves is rarely discussed in quantum mechanics, simply because the latter is not a matter for electrons, nucleon, or photons, but it is a matter in astrophysics. The analysis of observation data tells us that on the planetary scale, the coherence width of relativistic matter waves can be extended to 1000 kilometers or more, as illustrated in **Figure 5(a)**, the overlap may even occur in the width direction, thereby bringing new aspects to wave interference.

In the solar convective zone, adjacent convective arrays form a top-layer flow, a middle-layer gas, and a ground-layer flow, similar to the concept of **molecular current** in electromagnetism. Considering one convective ring at the equator as shown in **Figure 5(b)**, there is an apparent velocity difference between the top-layer flow and the middle-layer gas, where their relativistic matter waves are denoted respectively by

$$\begin{aligned} \psi &= \psi_{\text{top}} + C\psi_{\text{middle}} \\ \psi_{\text{top}} &= \exp\left[\frac{i\beta}{c^3}\int_L\left(v_1 \mathrm{d}l + \frac{-c^2}{\sqrt{1-v_1^2/c^2}}\mathrm{d}t\right)\right] \\ \psi_{\text{middle}} &= \exp\left[\frac{i\beta}{c^3}\int_L\left(v_2 \mathrm{d}l + \frac{-c^2}{\sqrt{1-v_2^2/c^2}}\mathrm{d}t\right)\right] \end{aligned} \tag{7}$$

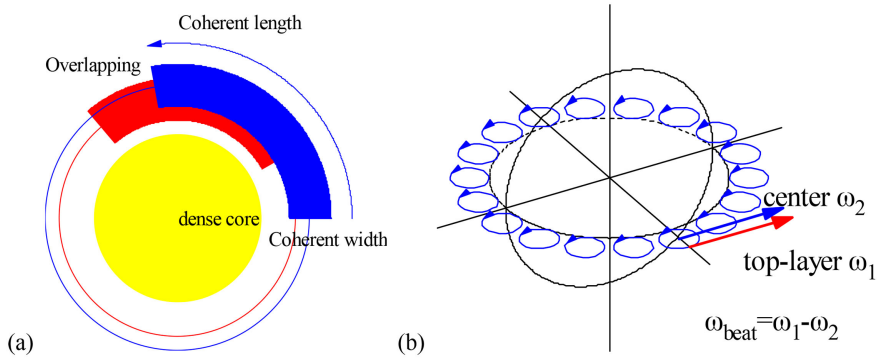

Figure 5. (a) Illustration of overlapping in the coherent width direction; (b) In convective rings at the equator, the speed difference causes a beat frequency.

Their interference in the coherent width direction leads to a beat phenomenon

$$\begin{aligned} &|\psi|^2 = |\psi_{\text{top}} + C\psi_{\text{middle}}|^2 = 1 + C^2 + 2C\cos\left[\frac{2\pi}{\lambda_{\text{beat}}}\int_L \mathrm{d}l - \frac{2\pi}{T_{\text{beat}}}t\right] \\ &\frac{2\pi}{T_{\text{beat}}} = \frac{\beta}{c^3}\left(\frac{c^2}{\sqrt{1-v_1^2/c^2}} - \frac{c^2}{\sqrt{1-v_2^2/c^2}}\right) \simeq \frac{\beta}{c^3}\left(\frac{v_1^2}{2} - \frac{v_2^2}{2}\right) \\ &\frac{2\pi}{\lambda_{\text{beat}}} = \frac{\beta}{c^3}(v_1 - v_2); \quad V = \frac{\lambda_{\text{beat}}}{T_{\text{beat}}} = \frac{1}{2}(v_1 + v_2) \end{aligned} \tag{8}$$

Their speeds are calculated as

$$\begin{aligned} &v_1 \approx 6100(\text{m/s}) \quad (\approx \text{observed in Evershed flow}) \\ &v_2 = \omega r_{\text{middle}} = 2017(\text{m/s}) \quad (\text{solar rotation}); \end{aligned} \tag{9}$$

where regarding Evershed flow as the eruption of the top-layer flow, about 6 (km/s) speed was reported [26]. Alternatively, the top-layer speed v_1 also can be calculated in terms of thermodynamics, to be v_1 = 6244 (m/s) [7]. Here using v_1 = 6100 (m/s), their beat period T_{beat} is calculated to be a very remarkable value of 10.93 (years), in agreement with the sunspot cycle value (say, mean 11 years).

$$T_{\text{beat}} \simeq \frac{4\pi c^3}{\beta\left(v_1^2 - v_2^2\right)} = 10.93(\text{years}) \tag{10}$$

The relative error to the mean 11 years is 0.6% for the beat period calculation using the relativistic matter waves. This beat phenomenon turns out to be a **nucleon density oscillation** that undergoes to drive the sunspot cycle evolution. The beat wavelength λ_{beat} is too long to observe, only the beat period is easy to be observed. As shown in **Figure 6**, on the solar surface, the equatorial circumference $2\pi r$ only occupies a little part of the beat wavelength, what we see is the expansion and contraction of the nucleon density.

$$\frac{2\pi r}{\lambda_{\text{beat}}} = 0.0031 \tag{11}$$

This nucleon density oscillation is understood as a new type of nuclear reaction on an astronomic scale.

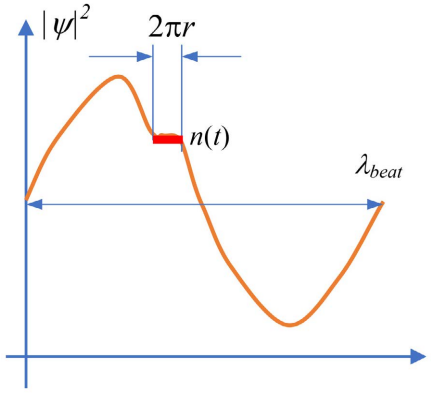

Figure 6. The equatorial circumference 2πr only occupies a little part of the beat wavelength, what we see is the expansion and contraction of the nucleon density.

In the above calculation, although this seems to be a rough model, there is an obvious correlation between solar radius, solar rotation, solar density, and solar constant β.

6. Atmospheric Circulation

Consider a relativistic matter wave ψ_A in the Earth shell at the latitude angle A, it will interfere with its neighbor waves within its coherent width. Because the Earth shell mainly consists of dense matter, their mutual cascade-interference will cause the relativistic matter waves to have the same phase at the same longitude, so that the relativistic matter wave ψ_A should equal to the ψ_{equator} at the same longitude, as shown in **Figure 7(a)**. This conclusion is supported by the spherical symmetry of the Earth's density distribution, that is

$$\begin{aligned} &\text{spherical symmetry: } \rho(r,A,\varphi)=\rho(r) \quad \Rightarrow \quad \psi(r,A,\varphi)=\psi(r) \\ &\text{or: } \psi_A=\psi_{\text{equator}} \end{aligned} \tag{12}$$

On the contrary, in the thin atmosphere, the cascade-interference within coherence width can be ignored, so the wind and clouds are widely distributed in the sky on a large scale.

Using the coherent width concept, considering the interference between the air ψ_A at the latitude angle A and the shell ψ_{shell} at the same latitude, their interference is

$$\begin{aligned} &\psi(r,A)=\psi_{\text{air}}(r,A)+C\psi_{\text{shell}}(r,A)=\psi_{\text{air}}(r,A)+C\psi_{\text{shell\_equator}}(r) \\ &T_{\text{beat}} \simeq \frac{4\pi c^3}{\beta\left(v_{\text{shell\_equator}}^2-v_{\text{air}}^2\right)} \\ &v_{\text{shell\_equator}}=\omega r \\ &v_{\text{air}}=\omega r\cos(A)+v_{\text{wind}}+v_{\text{sun\_effect}} \end{aligned} \tag{13}$$

where C represents the coupling constant which relates to their distance and mass fractions, their interference leads to a beat phenomenon. Positive wind represents

the direction from west to east. The air is subjected to the solar radiation which enforces the beat oscillation to run at the period $T_{\text{beat}} = 1$ (year) at the latitude angles $A = 23.5^{\circ}\text{S} - 23.5^{\circ}\text{N}$ due to the tilt of the Earth axis with respect to the Earth's orbital plane.

Suppose in spring the Sun directly shines on latitude $A_1 = 12^{\circ}\text{N}$ on the northern hemisphere, where the atmosphere undergoes a beat $T_{\text{beat}} = 1$ (year) with zero wind due to the constructive interference with the Sun. This mostly shined latitude A_1 is called as the first constructive interference ridge, with zero wind, using the above beat period formula we obtain the Sun effect

$$v_{\text{sun\_effect}} = 369.788 - \omega r \cos(A_1); \quad (\text{units}: \text{m/s}) \tag{14}$$

At the same time, the Sun effect at other latitude A should be

$$v_{\text{sun\_effect}} = 369.788 \cos(A - A_1) - \omega r \cos(A) \tag{15}$$

Thus, it follows the beat period formula that the wind under control of the beat T_{beat} is given by

$$v_{\text{wind}} = \sqrt{\omega^2 r^2 - \frac{4\pi c^3}{\beta T_{\text{beat}}}} - \omega r \cos(A) - v_{\text{sun\_effect}} \tag{16}$$

It is not easy to maintain the constructive interference condition for these waves. When the first constructive interference ridge is at latitude $A_1 = 12^{\circ}\text{N}$, the wind required for maintaining the beat $T_{\text{beat}} = 1$ (year) near the latitude $A = 12^{\circ}\text{N}$ is calculated by Equation (16) as shown in **Figure 8(a)** (blue line), this wind will be destroyed by destructive interference at higher latitudes. But, the wind will arise up again at the next locations where the waves again satisfy the constructive interference condition: at $A = 39^{\circ}\text{N}$ location (second ridge) where beat $T_{\text{beat}} = 0.5$ (years), and at $A = 57^{\circ}\text{N}$ location (third ridge) where beat $T_{\text{beat}} = 0.37$ (years) which is the shortest period that the Earth can get within the arctic regions. The maximal wind appears most probably at the midpoint of the first two ridges, about 48 (m/s). Linking all characteristic points in **Figure 8(a)** we obtain the predicted wind-curve over the northern hemisphere; this prediction agrees well with the experimental observations at an altitude of 10 km (200 hPa), as shown in **Figure 9**.

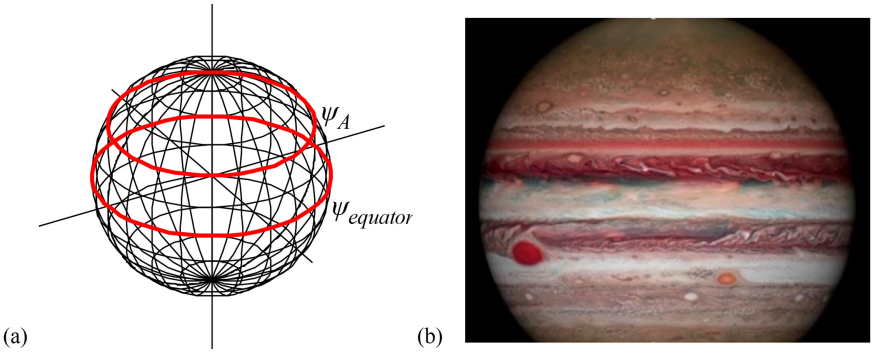

Figure 7. (a) Mutual cascade-interference will lead to the symmetry of the Earth's density distribution; (b) Zonal winds on Jupiter (the photo from public News).

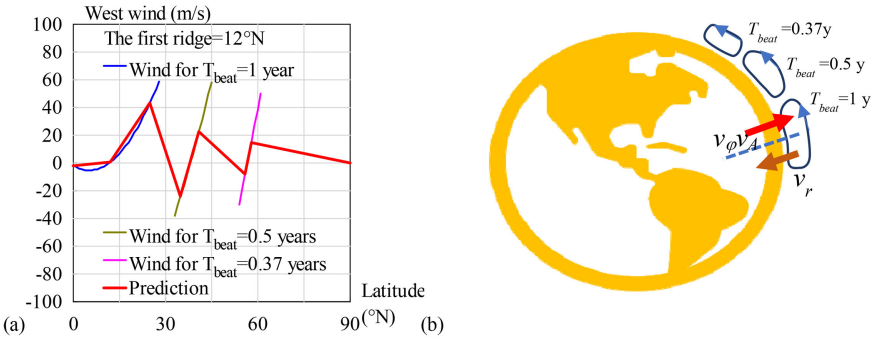

Figure 8. (a) Calculation of west winds in the northern hemisphere; (b) The atmospheric circulation in the northern hemisphere.

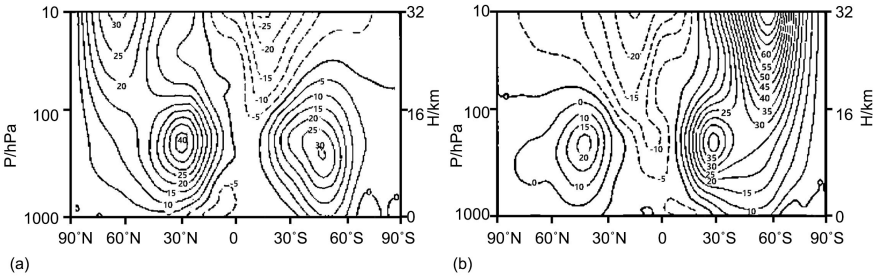

Figure 9. NCEP/NCAR data, mean west winds over 40 years (1958-1997) [27]. (a) Winter; (b) Summer.

<Clet2020 Script>//C source code

```
double beta,H,M,r,rc, rs, rot,v1,v2, Year,T,Lamda,V,a,b,w,Fmax,N[500],S[500],
F[100]; int i, j, k, t, m, n, s, f,Type,x;
int main(){beta=1.377075e+14; H=SPEEDC*SPEEDC*SPEEDC/beta;
M=5.97237e24; rs=6.371e6; rot=2*PI/(24*3600); Year=24*3600*365.2422;
Type=1; x=10; if(Type>1) x=-30;//v2=rs*rot; a=v2*v2-4*PI*H/Year; V=sqrt(a)-v2;
if(Type== 1) SetAxis(X_AXIS,0,0,90,"Latitude#n(˚N);0;30;60;90;");
else SetAxis(X_AXIS,-90,-90,90,"Latitude#n(˚N);=90;-60;-30;0;30;60;90;");
SetAxis(Y_AXIS,-100,-100,100,"West wind (m/s);-100;-80;-60;-40;-20;0;20;40;
60;80;100;");
DrawFrame(0x016a,Type,0xafffaf);//Polyline(2,"-90,0,90,0");
Check(15,k); if(k>24) k=24; if(k<-24) k=-24; //TextAt(100,10,"V=%f",V);
T=Year/2; Wind(); f=0; Findf(); t=N[m+m]; T=Year; Wind(); f=0; Findf();
SetPen(2,0xff); Polyline(n,N,x,70,"Wind for T#sdbeat#t=1 year"); if(Type>1)
Polyline(s,S);
F[0]=N[0];F[1]=N[1]; F[2]=N[m+m]; F[3]=N[m+m+1]; t=(t+F[2])/2;//midst
of two ridges
t=t-F[2]+m; Fmax=N[t+t+1]; //TextAt(100,20,"t=%d, Fmax=%f ",t,Fmax);
f=Fmax; Findf(); F[4]=N[m+m]; F[5]=N[m+m+1];
T=Year/2; Wind(); f=-Fmax/2; Findf(); t=m;f=Fmax/2; Findf();
SetPen(2,0x80ff00); Polyline(n,N,x,-50,"Wind for T#sdbeat#t=0.5 years");
if(Type>1) Polyline(s,S);
```

```
F[6]=N[t+t]; F[7]=N[t+t+1]; F[8]=N[m+m]; F[9]=N[m+m+1];
T=0.37*Year; Wind(); f=-Fmax/4; Findf(); t=m;f=Fmax/4; Findf();
SetPen(2,0x9933fa); Polyline(n,N,x,-70,"Wind for T#sdbeat#t=0.37 years");
if(Type>1) Polyline(s,S);
F[10]=N[t+t]; F[11]=N[t+t+1]; F[12]=N[m+m]; F[13]=N[m+m+1]; F[14]=90;
F[15]=0;
//Draw("ELLIPSE,0,2,XYX,10","15,20,25,35");TextHang(5,40,0,"a route");
SetPen(3,0xff0000); Polyline(8,F,x,-90,"Prediction"); TextHang(x,90,0,"The
first ridge=%d°N", k);
}
Wind(){n=0;s=0;
for(i=0;i<90;i+=1) { a=i*PI/180; b=(i-k)*PI/180; v1=rot*rs*cos(a); v2=rot*rs;
w=369.788*cos(b)-v2*cos(k*PI/180); a=v2*v2-4*PI*H/T; V=sqrt(a)-v1-w;
if(V>-40 && V<60) {N[n+n]=i; N[n+n+1]=V; n+=1;}}
for(i=0;i<90;i+=1) { a=-i*PI/180; b=(-i-k)*PI/180; v1=rot*rs*cos(a); v2=rot*rs;
w=369.788*cos(b)-v2*cos(k*PI/180); a=v2*v2-4*PI*H/T; V=sqrt(a)-v1-w;
if(V>-40 && V<60) {S[s+s]=-i; S[s+s+1]=V; s+=1;}} }
Findf(){a=1e10;for(i=0;i<n;i+=1){b=N[i+i+1]-f;if(b<0) b=-b;if(b<a) {m=i;a=b;}}
}//if(k== 12) ClipJob(APPEND,"i=%d,V=%f",i,V);
#v07=?>A
```

For further improvement of precision, the value of the wind required by the constructive interference condition should be understood as a magnitude, it should be resolved into three components in the spherical coordinates (r, A, φ) as

$$v_{\text{wind}}^2 = v_r^2 + v_A^2 + v_\varphi^2 \tag{17}$$

According to the energy equipartition theorem in thermodynamics, approximately we have the average estimation

$$\left\langle v_r^2 \right\rangle = \left\langle v_A^2 \right\rangle = \left\langle v_\varphi^2 \right\rangle = \frac{1}{3} v_{\text{wind}}^2 \tag{18}$$

Thus, the wind vectors around the northern hemisphere of the Earth are plotted in Figure 8(b), where the atmospheric circulation consists of three cells: Hadley cell, Ferrel cell, and arctic cell.

The beat $T_{\text{beat}} = 1$ (years) works out **two seasons** in the equatorial regions. The beat $T_{\text{beat}} = 0.5$ (years) blows comfortable winds over Europe, Northern America and Northeastern Asia, and modulates out **four seasons**; the shortest beat $T_{\text{beat}} = 0.37$ (years) has a beat wavelength too long to be confined in the arctic regions so that it escapes from the north pole toward the equator, so recognized as the planetary scale waves or **Rossby waves**; in other words, the arctic regions can contain $T_{\text{beat}} = 1/3$ (years) while emitting extra cold streams per 2.24 years to Europe, Northern America and Northeastern Asia.

Since the relativistic matter wave of the air interferes with the relativistic matter wave of the Earth shell, the easterlies at the equator have a magnitude of about 10 m/s in Figure 8(a). The trade winds or easterlies are the permanent east-to-west

prevailing winds that flow in the Earth's equatorial region. The trade winds blow mainly from the northeast in the Northern Hemisphere and the southeast in the Southern Hemisphere, strengthening during the winter and when the Arctic oscillation is in its warm phase. Trade winds have been used by captains of sailing ships to cross the world's oceans for centuries. The driving force of atmospheric circulation is the uneven distribution of solar heating across the Earth, which is greatest near the equator and least at the poles. This air rises to the tropopause, about 10 - 15 kilometers above sea level, where the air is no longer buoyant [28].

As we have known that $v_{\text{sun\_effect}} = -84$ (m/s) at the equator when the first constructive interference ridge at $A_1 = 12^{\circ}$N, imagine if nuclear wars happen on the Earth to stop the solar radiation to the Earth's surface, then the equatorial wind on the Earth's surface will simply reach to −94 (m/s), like the winds on the surfaces of Jupiter and Saturn, this will change global climate mode, killed all dinosaurs by strong winds and dusts. Thinking about Mars, Jupiter, and Saturn that gain very weak solar radiation, and there are at least 100 (m/s) strong zonal winds on their surfaces, as shown in **Figure 7(b)**. This section helps us understand how the dinosaurs to be buried.

7. Discussion

Although most astronomers think the Bode's rule does not express a broader universal law, this paper points out there is a relativistic matter wave in the solar system which undergoes to support the planetary orbital quantization pattern. In terms of the relativistic matter wave, the Sun and Earth are quantized in the central state $n = 0$ in manner of the multi-wavelet interference. If the first minimum of the interference in radius direction is defined as the location of true radius, then the true radius formula is given by

$$\delta = \frac{2\pi\beta\omega r^2}{c^3} = \frac{2\pi}{N}; \quad \Rightarrow \quad r = \sqrt{\frac{c^3}{\beta\omega N}}; \quad N = \sqrt{\frac{\rho_{\text{core}}}{\rho_{\text{surface\_gas}}}} \tag{19}$$

<Clet2020 Script>//C source code [29]

```
int N; double beta,H,M,r, rs, omega,atm_height;
main(){rs=6.95e8; omega=2*PI/(25.05*24*3600); N=sqrt(1408/0.004); beta=2.961520e+10;
H=SPEEDC*SPEEDC*SPEEDC/beta;
r=sqrt(H/omega*N); atm_height=r-rs; TextAt(100,100,"r=%e m, atm.=%e m",r,atm_height);
rs=6.378e6; N=sqrt(5530/1.29); omega=2*PI/(24*60*60); beta=1.377075e+14;
H=SPEEDC*SPEEDC*SPEEDC/beta;
r=sqrt(H/omega*N); atm_height=r-rs; TextAt(100,200,"r=%e m, atm.=%e m",r,atm_height);
}#v07=?>A
```

Theoretically, the solar true radius is 7.27e+8 (m), the Earth's true radius is 6.43e+6 (m).

The solar constant β = 2.961520e+10 (m/s^2) is obtained from the Sun, Mercury, Venus, Earth and Mars; therefore, if the Bode's rule holds, the solar radius is fixed and cannot be varied simply by solar nuclear reactions, temperatures, and pressures, it concerns with the Mercury, Venus, Earth and Mars.

The Earth constant β = 1.377075e+14 (m/s^2) is obtained uniquely from the line connecting the Earth and Moon in **Figure 3**. Human exploration to the Moon may cause severe impact on the Earth through the following technical route, this is a good excuse for stopping landing on the Moon for the security of the whole human.

$$\text{Human exploration} \Rightarrow H \uparrow\downarrow \Rightarrow |\psi|^2 \uparrow\downarrow \Rightarrow r \uparrow\downarrow \tag{20}$$

This discovery provides a rule to assess the solar and Earth's inner structure and their evolution.

8. Conclusion

In recent years, relativistic matter waves have been applied to the solar system to explain some quantum gravity effects. Since Bode's rule holds, there must exist a planetary wave called as relativistic matter wave to support its quantization pattern. This paper shows that the solar size and Earth's size are the consequences of Bode's rule in terms of the relativistic matter wave. The solar radius is determined as 7e+8 (m) with a relative error of 0.72%; the Earth's radius is determined as 6.4328e+6 (m) with a relative error of 0.86%. The Earth's atmospheric circulation is also investigated in terms of the relativistic matter wave, the wind fields on the Earth's surface are calculated, and the results agree well with experimental observation. These findings indicate that the solar system is under the control of the planetary relativistic matter waves.

Conflicts of Interest

The author declares no conflicts of interest regarding the publication of this paper.

References

[1] Marletto, C. and Vedral, V. (2017) Gravitationally Induced Entanglement between Two Massive Particles Is Sufficient Evidence of Quantum Effects in Gravity. *Physical Review Letters*, **119**, Article ID: 240402. https://doi.org/10.1103/PhysRevLett.119.240402

[2] Guerreiro, T. (2020) Quantum Effects in Gravity Waves. *Classical and Quantum Gravity*, **37**, Article ID: 155001. https://doi.org/10.1088/1361-6382/ab9d5d

[3] Carlip, S., Chiou, D., Ni, W. and Woodard, R. (2015) Quantum Gravity: A Brief History of Ideas and Some Prospects. I*nternational Journal of Modern Physics D*, **24**, Article ID: 1530028. https://doi.org/10.1142/S0218271815300281

[4] Schneider, S.E. and Arny, T.T. (2018) Pathways to Astronomy. 5th Edition, McGraw-Hill Education, London.

[5] De Broglie, L. (1923) Waves and Quanta. *Nature*, **112**, 540.

https://doi.org/10.1038/112540a0

[6] De Broglie, L. (1925) Recherches sur la théorie des Quanta. *Annales de Physique*, **10**, 22-128. https://doi.org/10.1051/anphys/192510030022

[7] Cui, H.Y. (2021) Relativistic Matter Wave and Quantum Computer. Kindle Ebook. Amazon, Seattle.

[8] The Solar Interior. NASA. https://solarscience.msfc.nasa.gov/interior.shtml

[9] Guenther, D.B., Demarque, P., Kim, Y.-C. and Pinsonneault, M.H. (1992) Standard Solar Model. *The Astrophysical Journal*, **387**, 372-393. https://doi.org/10.1086/171090

[10] Valencia, D., Sasselov, D.D. and O'Connell, R.J. (2007) Radius and Structure Models of the First Super-Earth Planet. *The Astrophysical Journal*, **656**, 545-551. https://doi.org/10.1086/509800

[11] Valencia, D., Sasselov, D.D. and O'Connell, R.J. (2007) Detailed Models of Super-Earths: How Well Can We Infer Bulk Properties? *The Astrophysical Journal*, **665**, 1413-1420. https://doi.org/10.1086/519554

[12] Guillot, T. and Showman, A.P. (2002) Evolution of "51 Pegasus b-Like" Planets. *Astronomy & Astrophysics*, **385**, 156-165. https://doi.org/10.1051/0004-6361:20011624

[13] Guillot, T. and Showman, A.P. (2002) Atmospheric Circulation and Tides of "51 Pegasusb-Like" Planets. *Astronomy & Astrophysics*, **385**, 166-180. https://doi.org/10.1051/0004-6361:20020101

[14] Fletcher, L.N., Kaspi, Y., Guillot, T. and Showman, A.P. (2020) How Well Do We Understand the Belt/Zone Circulation of Giant Planet Atmospheres? *Space Science Reviews*, **216**, Article No. 30. https://doi.org/10.1007/s11214-019-0631-9

[15] Kaspi, Y., Galanti, E., Showman, A.P., Stevenson, D.J., Guillot, T., Iess, L. and Bolton, S.J. (2020) Comparison of the Deep Atmospheric Dynamics of Jupiter and Saturn in Light of the Juno and Cassini Gravity Measurements. *Space Science Reviews*, **216**, Article No. 84. https://doi.org/10.1007/s11214-020-00705-7

[16] Orbital Debris Program Office (2018) History of On-Orbit Satellite Fragmentations. 15th Edition, National Aeronautics and Space Administration, Washington DC.

[17] Mulrooney, M. (2007) The NASA Liquid Mirror Telescope. Orbital Debris Quarterly News.

[18] Orbital Debris Program Office (2007) Chinese Anti-Satellite Test Creates Most Severe Orbital Debris Cloud in History. Orbital Debris Quarterly News.

[19] Manis, A., Matney, M., Vavrin, A., Gates, D., Seago, J. and Anz-Meador, P. (2021) Comparison of the NASA ORDEM 3.1 and ESA MASTER-8 Models. Orbital Debris Quarterly News.

[20] Wright, D. (2007) Space Debris. *Physics Today*, **10**, 35-40. https://doi.org/10.1063/1.2800252

[21] Tang, Z.-M., Ding, Z.-H., Dai, L.-D., Wu, J. and Xu, Z.-W. (2017) The Statistics Analysis of Space Debris in Beam Parking Model in 78˚ North Latitude Regions. *Space Debris Research*, **17**, 1-7. (In Chinese)

[22] Tang, Z.-M., Ding, Z.-H., Yang, S., Dai, L.-D., *et al.* (2018) The Statistics Analysis of Space Debris in Beam Parking Model Based on the Arctic 500 MHz Incoherent Scattering Radar. *Chinese Journal of Radio Science*, **25**, 537-542. (In Chinese)

[23] Tang, Z.-M., Ding, Z.-H., Dai, L.-D., *et al.* (2018) Comparative Analysis of Space Debris Gaze Detection Based on the Two Incoherent Scattering Radars Located at 69N and 78N. *Chinese Journal of Space Science*, **38**, 73-78. (In Chinese)

[24] Ding, Z.-H., Yang, S., Jiang, H., *et al.* (2018) The Data Analysis of the Space Debris Observation by the Qujing Incoherent Scatter Radar. *Space Debris Research*, **18**, 12-19. (In Chinese)

[25] Yang, S., Ding, Z.-H., Xu, Z.-W. and Wu, J. (2018) Statistical Analysis on the Space Posture, Distribution, and Scattering Characteristic of Debris by Incoherent Scattering Radar in Qujing. *Chinese Journal of Radio Science*, **33**, 648-654. (In Chinese)

[26] Cox, A.N. (2001) Allen's Astrophysical Quantities. 4th Edition, Springer, New York. https://doi.org/10.1007/978-1-4612-1186-0

[27] Li, L.P., *et al.* (2021) Introduction to Atmospheric Circulation. 2nd Edition, Science Press, Beijing. (In Chinese)

[28] Atmosphere of Earth. Wikipedia. https://en.wikipedia.org/wiki/Atmosphere_of_Earth

[29] Clet Lab (2022) Clet: C Compiler. https://drive.google.com/file/d/1OjKqANcgZ-9V56rgcoMtOu9w4rP49sgN/view?usp=sharing